Dynamic Site Characterization of Areas affected by the 2017 Puebla-Mexico City Earthquake

Clinton M. Wood[a*], Michael Deschenes[a], Christian Ledezma[b], Jorge Meneses[c], Gonzalo Montalva[d], Alesandra C. Morales-Velez[e]

[a] *Dept. of Civil Eng.,University of Arkansas, Fayetteville, Arkansas, United States*
[b] *Dept. of Struct. And Geotech. Eng., Pontificia Universidad Católica de Chile, Santiago, Chile*
[c] *California Seismic Safety Commission, San Diego, California, United States*
[d] *Dept. de Ing. Civil, Universidad de Concepción, Concepción, Chile*
[e] *Dept. of Civil Eng. and Survey, University of Puerto Rico Mayaguez, Mayaguez, Puerto Rico*

Abstract

Dynamic site characterization was conducted using the microtremor and earthquake horizontal to vertical spectral ratio methods (MHVSR and EHVSR) and surface wave methods at locations affected by the 2017 Mw 7.1 Puebla-Mexico City Earthquake. These data were compared to published results to understand the accuracy of currently available dynamic site information including site period maps and Vs profiles. Results indicate the current Mexican design code site period map, NTC [9], provides superior estimates of microtremor site periods in Mexico City compared to maps published by Lermo and Chávez-García [7] and Arroyo et al. [11]. However, the NTC [9] map still had significant errors of 15-30% between the estimated and measured site periods, but only had an average bias of 5%. Moreover, the changes in site period within the Mexico basin due to groundwater withdrawal and consolidation of the lacustrine clay deposits were shown to be progressing faster than originally estimated by Arroyo et al. [11].

Keywords: [Horizontal to Vertical Spectral Ratio; Dynamic Site Characterization; Mexico City; Site Period; Puebla-Mexico City Earthquake]

1.0 Introduction

The recent September 19, 2017, Mw 7.1 Puebla-Mexico City earthquake caused widespread damage in the central region of Mexico [1]. Significant effects were observed across the states of Puebla, Morelos, Mexico, and others with strong ground shaking in Mexico City despite being located approximately 120 km from the epicenter. Observations from previous earthquakes in 1957, 1979, 1985,

*Corresponding author. +1 479 575 6084
E-mail addresses: cmwood@uark.edu (C. Wood), mrdesche@email.uark.edu (M. Deschenes), ledezma@ing.puc.cl (C. Ledezma), jmenesesl@gmail.com, (J. Meneses), gmontalva@udec.cl (G. Montalva), alesandra.morales@upr.edu (A. Morales)

and 1999 have unveiled the regional and local complex geologic, geotechnical, and hydrological settings in and around Mexico City [2, 3]. In particular, Mexico City sits on the sediments of the former Texcoco and Xochimilco-Chalco Lakes that disappeared due to groundwater extraction and land reclamation. The sediments comprise a relatively shallow layer (≤ 50 m) of unconsolidated lacustrine clay with shear wave velocity, $Vs \leq 100$ m/s [3,4], underlain by thin layers of dense sand and stiffer clays [5]. The areas surrounding the lake zone, known as the transition zone, are composed of weathered rock or hard soil deposits with Vs ≥ 450–600 m/s; beyond which lies the hill zone, mostly composed of volcanic rocks. The impedance contrast of the unconsolidated sediments in the lake zone and the underlying and surrounding stiffer soils, sand layers, and volcanic rocks, create a unique and complex setting for ground shaking amplification due to site effects. Each of the past earthquakes in central Mexico has shown the ground motions induced by the earthquakes that have affected with different intensities the built environment and people according to the unique and rapidly changing subsurface conditions in Mexico City and the surrounding areas. The spatial distribution of damage to the built environment has reflected not only the condition of the structures affected but most important the local site conditions (i.e., thickness of the clay deposit), extent of the basin underneath the lake clay deposits, and the location of the earthquake source.

The distance of the seismic sources, the thickness of the soil deposit, and the height of the buildings are related to the level of seismic demand and resulting damage to buildings in Mexico City (Fig. 1). The more distant subduction events (1985 earthquake) are richer in longer periods (T_{SWD}) or low frequencies; the closer intraplate events (1999 and 2017 earthquakes) are richer in short periods (T_{SWN}) or high frequencies [1]. The thickness of the soil deposit plays an important role in the fundamental period (T_S) of the soil deposit. The thicker the soil deposit, the longer the vibration period; the thinner the soil deposit, the shorter the vibration period. Moreover, the fundamental period of a building (T_b) is controlled by the height of the building. The taller the building, the longer the fundamental period; the shorter the building, the shorter the fundamental period.

The spatial extent of the building damage in and around Mexico City is primarily controlled by these three periods: (1) predominate period of seismic waves, (2) soil deposit thickness, and (3) height of the buildings [6]. When the three fundamental periods approximately match, the seismic demand to buildings is the largest due to the effect of double resonance ($T_{sw} \approx T_S \approx T_b$). Distant subduction fault sources generate longer periods (T_{SWD}) that may match the fundamental periods of relatively deep deposits (T_{s2}). Under this scenario, buildings with fundamental periods (T_{b2}) close to the soil period (T_{s2}) experience the largest seismic demand. On the other hand, nearby intraplate fault sources generate shorter periods (T_{SWN}) that match with the fundamental periods of relatively shallow deposits (T_{s1}). Under this scenario, buildings with fundamental periods (T_{b1}) close to the soil period (T_{s1}) experience the largest seismic demand.

Therefore, the damage from each earthquake tracks very well with the period of the soil deposits under Mexico City.

Because of the strong correlation between observed damage and the natural period of the soil deposit in Mexico City, extensive site period characterization using microtremor horizontal to vertical spectral ratio (MHVSR) has been conducted in the Mexico City area by numerous researchers [7,8,9,10,11]. These researchers have used these extensive measurements to develop site period contour maps of the Mexico City Basin [7,9,11] and have even incorporated these maps into the seismic design code for Mexico City [9]. In addition to site period measurements, measurement of shear wave velocities has been completed by a number of researchers [4,5,12], who showed the extremely soft nature of the unconsolidated lacustrine clay with Vs less than 100 m/s. These soil deposits tend to amplify ground motions around the natural period of the deposits as discussed above and therefore play a critical role in understanding the seismic hazard of the region. Moreover, due to excessive groundwater extraction from the Mexico City basin, there is now a 24% deficit between the water recharge rate and the withdrawal rate from the basin [11]. This deficiency in water recharge has contributed to the consolidation of the aquitards underlying the city, causing exceptional ground subsidence levels at rates of 5–40 cm/year [11]. This consolidation has also been linked to a site period change over time under different portions of the city [11]. Arroyo et al. [11] developed site period maps based on site period measurements and previous measurements of the thickness of the lacustrine clay deposit which represent the basin site period from 1985 and 2010, then used the rate of subsidence to extrapolate a future site period map for the year 2050. Based on the constantly changing site period in the basin, there is a need to understand the accuracy of currently available dynamic site characterization information in the Mexico City region and how the change in site period will occur over time.

This paper presents dynamic site characterization of areas affected by the 2017 Puebla-Mexico City earthquake with sites located within Mexico City and west and south of Mexico City in Jojutla and Puebla. Site periods were measured and computed using the horizontal to vertical spectral ratio method using microtremors (MHVSR) and earthquake records (EHVSR) from strong motion stations. Active and passive surface waves measurements were made using the multichannel analysis of surface waves (MASW) and microtremor array measurements (MAM) methods. These data are compared to the known geologic and geo-seismic conditions within the region to understand trends in the data. The measured site periods in Mexico City are then compared to previously published site period contour maps by Lermo and Chávez-Garcia [7], NTC [9], and Arroyo et al. [11] to understand the accuracy of these site period maps and understand any potential bias in the data, and they are used to understand the rate at which the site periods

are changing within the basin. Finally, the Vs profiles developed from surface wave methods are presented and compared to available data in the Mexico City Basin.

2.0 Site Period and Surface Wave Measurements in Mexico City and Surrounding Areas

Microtremor site period measurements were made using the MHVSR method [13,14,15] in Mexico City at 18 locations by the GEER advanced team (Universidad de Concepción and Pontificia Universidad Católica de Chile, UdeC-PUC) and at 13 locations by the GEER main team (University of Arkansas, Uark). As shown in Fig. 2 and tabulated in Table 1, the majority of these measurements were made in the western portion of Mexico City near the transition between Zones II and III [9] with five additional measurements made in the southern portion of the city. The motivation for making these measurements was to validate the Mexico City site period zonation map and estimate site periods for areas affected by the earthquake. In addition to measurements in Mexico City, 10 site period measurements were made to the South and East of Mexico City in locations closer to the epicenter (i.e., Jojutla and Puebla, see Fig. 2).

The equipment used to collect the MHVSR measurements consisted of triaxial Tromino® seismometers (0.3 Hz or less [16] used by the UdeC-PUC team and a Nanometrics Trillium Compact (100-0.05 Hz sensor) three component broadband seismometer and Centaur digitizer used by the Uark team. Microtremor energy (noise) was recorded for between 15-120 minutes at each location. A typical MHVSR field setup is shown in Fig. 3b. Data analysis was performed in Geopsy according to the general guidelines developed by the SESAME project [14,17]. The time records were divided into 60-120 second blocks for processing. Time windows with excessive noise were rejected. The Fourier spectra of the remaining time windows were computed and then smoothed using a Konno-Ohmachi filter. These spectral estimates were used to compute the MHVSR for each window and a spectral average of all the time windows was used to represent the response of each station. In addition to MHVSR measurements, earthquake HVSR (EHVSR) were computed for strong motion station (SMS) records from the 2017 Puebla-Mexico City main shock. The locations of the SMS in Mexico City are tabulated in Table 2. The EHVSR were computed using the entire ground motion record and smoothed using a Konno-Ohmachi filter.

In addition to MHVSR and EHVSR measurements, active and passive surface wave measurements were made at 5 locations (see Table 1) where site period measurements were made. These locations were primarily in Mexico City with one location in Puebla, as shown in Fig. 2. The surface wave measurements consisted of active Multichannel Analysis of Surface Waves (MASW) and Passive Microtremor Array Measurements (MAM) [18, 19]. The active MASW measurements utilized a linear array of 24, 4.5 Hz vertical geophones with a uniform spacing between geophones of 2 meters. Rayleigh type surface waves were generated using a 4 kg sledgehammer with source locations of 5, 10, and 20 meters from the first

geophone in the array. Multiple source offsets were used to ensure high quality data, allow uncertainty to be estimated, and ensure near-field effects do not corrupt the data. The surface wave propagation was recorded using a Geometrics Geode seismograph. At each source location 10 sledgehammer blows were stacked to increase the signal to noise ratio of the recorded signals. A typically MASW field setup at the Escocia site is shown in Fig. 3a and 3c.

The active source data was analyzed using the frequency domain beamformer (FDBF) method [20] coupled with the multiple source-offset technique for identifying near-field contamination and quantifying dispersion uncertainty [21]. Dispersion data were generated from each source-offset location (i.e., 5, 10, and 20 meters), and the maximum spectral peak for each frequency was picked automatically in Matlab. The individual dispersion data from each source offset were combined to form a composite dispersion curve. After eliminating clear near-field data, the composite experimental dispersion curve was divided into 100 frequency bins spaced equally between 1 to 100 Hz according to a log scale. The mean phase velocity and associated standard deviation were then calculated for each bin, resulting in an experimental dispersion curve with associated uncertainty for each frequency.

Passive MAM were conducted using an L-shaped array of 24, 4.5 Hz vertical geophones with a spacing of between 4-5m between geophones depending on the available space at each particular site. Passive energy from urban noise or environmental energy from wind or other sources was utilized for the testing. The surface wave propagation was recorded using a Geometrics Geode seismograph. A total of 30, 60 second records were recorded at each site for a total recording time of 30 minutes. A typical MAM field setup is shown in Fig. 3a. The MAM data were analyzed using the 2D frequency-wavenumber method as programmed in the Geopsy software [17]. Dispersion uncertainty was estimated by processing the time records in 60 second blocks. The phase velocities obtained from each block were used to obtain a mean and standard deviation at each frequency. The composite experimental dispersion curve was divided into 100 frequency bins equally spaced between 1 to 30 Hz on a log scale. Similar to the active source data, the mean phase velocity and associated standard deviation were calculated for each bin.

Once the Rayleigh wave dispersion estimates were obtained, an inversion was performed using either the multi-modal joint inversion (Rayleigh dispersion and HVSR site period) in Geopsy alone or in combination with WinSASW. WinSASW was used exclusively for sites which had high velocity crustal layers and softer layers underneath. These sites could not be inverted using the Geopsy software alone due to problems with the inversions calculations. For the Geopsy inversions, the Rayleigh dispersion data and HVSR peak were jointly inverted. Layer interfaces were only loosely constrained and allowed to find any appropriate depth. If layering information from invasive tests were available, these were used to constrain/inform the layering of the site. The shear wave velocities of each layer were constrained within

reasonable velocities for geotechnical materials, which were defined as a function of material type and confining pressure. However, the clays in Mexico City are known to be significantly softer than typical materials [4]. Poisson's ratio was allowed to vary between 0.25-0.50 except where the location of the water table was known in which case the P-wave velocity was fixed at 1500 m/s. The density was varied for each layer from 1600-2000 kg/m3 depending on the estimated Vs of the layer. Multiple inversion analyses with varying parameters (thickness/Vs and number of layers) were conducted for each site to ensure parameterization choices did not negatively influence the results Vs profile. The neighborhood algorithm in Geopsy [17] was used to search approximately 1 million models in each analysis. The relative quality of fit was quantified by the minimum misfit, which compares the theoretical data to the experimental data in terms of the collective squared error. In addition, the dispersion and site period fits were compared by visual observation to ensure the highest quality fit was obtained [22, 23].

For dispersion data inverted in combination with WinSASW, Rayleigh dispersion data was fit by eye using the 2D theoretical solution. Poisson's ratio was set to 0.3 except where the location of the water table was known in which case the P-wave velocity was fixed at 1500 m/s. The density of each layer was based on the suspected material type and shear wave velocity. The near surface layering (high frequency dispersion data) was then forced in the Geopsy inversion to insure the near surface layering is properly considered in the final Vs profile development.

3.0 Site Period Results from MHVSR and EHVSR Measurements

3.1 MHVSR Site Period Measurements Comparison to Geologic Conditions

A comparison of the MHVSR site period estimates and geologic conditions from the Instituto Nacional de Estadística y Geografía (INEGI) is presented in Fig. 2. The MHVSR site periods measured at each location are tabulated in Table 1. In and around the Mexico City area, the site periods correlate well with the alluvial soils known to exist in Mexico City with site periods near or exceeding 1.0 seconds. As one transitions south of Mexico City, the measured site periods are in general agreement with the published geologic conditions (alluvial deposits) with the Yautepec Bridge and the Jojutla sites having longer periods of 0.83 sec and 0.27 sec, respectively. Other sites with relatively short site periods (<0.25 sec) or no resolved site period correspond to locations where limestone or igneous rock is expected. The Cuernavaca site is the outlier with a relatively long period of 1.14 sec, but is located on igneous rock formations, which does not correlate with the longer site period. This long period may be caused by deeper basement rock or potential errors in the measurement. The relatively short site period recorded at Jojutla likely contributed to the significant damage observed in short period structures within that town [24]. Comparing the site period measurements for the City of Puebla to the geologic conditions, the Calle 6 and City Plaza locations have

site periods of 0.89 sec and 0.78 sec, respectively. Although these measurements match well with previous measurements made by [25] with site periods in the city center between 0.75 sec and 1.0 sec, the sites are located on igneous rock conditions according to the geologic map. This suggests that some soil or other impedance contrast must exist under the city center which influences the potential site effects in the area. In contrast to the city center sites in Puebla, the Cactopea site to the southwest of the city center had no measurable site period, which would be expected given the igneous rock conditions at the site.

3.2 MHVSR and EHVSR Site Period Measurements in Mexico City

The MHVSR and EHVSR site period estimates in Mexico City are tabulated in Table 1 and 2 and shown in Fig. 4 along with the geo-seismic zonation map from NTC [9]. The site periods across Mexico City vary significantly within a short distance (~ 17 km), from 0.73 sec at the edge of the basin to 5.1 sec in the center of the basin. In general, the site period measurements agree very well with the geo-seismic zonation map with periods less than 1.0 sec typically observed in Zones I and II and those greater than 1.0 sec in the various Zone III categories. One of the lone outliers is Station TP13 on the southwest side of the city with a site period of 4.0 sec in Zone I. This may be the result of an impedance contrast in the deeper subsurface below the volcanic rock, but no other stations recorded a similar long site period in Zone I. Nearby stations FJ74 and CUP5 have site periods of 1.3 seconds, which are longer than expected for Zone I. In general, Zone I and II generally have site periods less than 1.0 sec, Zone IIIa has site periods between 1-1.5 sec, Zone IIIb has site periods between 1.5-2.0 sec, Zone IIIc has site periods between 2.0-3.0 sec, and Zone IIId has site periods greater than 3.0 sec. Comparing the western edge of the basin (bottom subfigure), the basin seems to make a smooth, but very rapid change in site period from a period of 1.21 sec to 0.73 sec over about a 2 km region, which emphasizes the steep edge of the basin in that region of Mexico City.

To better understand the changes in site period across the basin in comparison to previous site period measurements, Fig. 5 compares the MHVSR and EHVSR site periods, the site period contour maps produced by Lermo and Chávez-Garcia [7] referred to as L&C-1994, NTC [9] referred to as NTC-2004, and Arroyo et al. [11] (2010 estimate) referred to as AEA-2010. The measurement locations are colored in each figure based on the error between the estimated contour map site periods and the measured site periods. The contour map periods were estimated for each of the measurement locations based on a nearest neighbor calculation scheme where the nearest distance to contour lines on either side of each measurement point was used to estimate the site period based on linear interpolation. For measurement locations outside the shortest period contour line, the site period could not be estimated and is therefore shown in black and excluded from future calculations. The percent difference between the measured site period and the estimated site period for each location and contour map was computed as the estimated period minus the

measured period divided by the measured period. Therefore, blue points represent locations where the estimated period is shorter (stiffer or underestimate) than the observed measurement by more than 10% while the red points represent locations where the estimated period is longer (softer or overestimate) than the observed measurement by more than 10%. Estimated points within 10% of the measured value are considered to be within a reasonable range of accuracy and therefore colored green. A 10% change is believe to represent a true difference between the measured and estimated results as the uncertainty in the estimated and measured site periods are believed to be within 5-10% of the true values. One item to note is that the site period contour maps were generated in different years for each study (i.e., 1994, 2004, and 2010, respectively). While in most areas this would not represent an issue, excessive groundwater withdrawal from the basin is believed to be causing a shift in the site period across the basin due to consolidation of the lacustrine clay deposit [11]. The site periods are believed to be getting shorter with time as the clay consolidates due to the ground water extraction. This will be discussed further later in the paper, but is expected to play a role in the differences between the contour maps.

For the L&C-1994 map in Fig. 5, the estimates from the contour map tend to either overestimate the period (too soft) or be with 10% for the western edge of the basin where the highest concentration of site period measurements are available. In general, the maps tends to underestimate (too stiff) the site period in the northern portion of the basin and the southwestern portion between the former Texcoco and Xochimilco-Chalco Lakes. The L&C-1994 tends to overestimate (too soft) or correctly estimate site periods within the former Xochimilco-Chalco Lake. Similar to the L&C-1994 contour map, the NTC-2004, developed 10 years later, tends to overestimate (too stiff) or correctly estimate site period in the central portion of the basin in geo-seismic zone III especially toward the western edge. In zone II, on the western edge of the basin, the NTC-2004 map tends to underestimate (too stiff) many of the sites periods in that area. This means that over the 10 year period from 1994 to 2004 the estimated site periods tended to get shorter (i.e., stiffer) based on a comparison of the L&C-1994 and NTC-2004 contour maps. However, the measured values seem to indicate that the 2017 site periods in the basin are in general softer (i.e., longer measured site periods compared to the estimated site periods) in zone II. Finally, the AEA-2010 contour map tends to overestimate (too soft) or correctly predict the site periods on the western edge of the basin similar to the L&C-1994 contour map and underestimate (too stiff) the site periods in other portions of the basin similar to the NTC-2004 contour map.

To better understand the potential bias between the measured site periods and the previously developed contour maps, Fig. 6 compares the measured site periods against the estimated periods for each measurement point and contour map. The MHVSR and EHVSR site period points are separated to understand any potential bias that may exist between these measurement methods. For each of the

comparisons, the majority of the MHVSR points are concentrated in the short period range between 0.5-2.0 sec, while the EHVSR measurements are spread over a larger period range from 0.5-5.1 sec. This is a limitation of the current MHVSR dataset.

Comparing the L&C-1994 estimates to the measured site periods in Fig. 6a, the MHVSR points show a bias toward overestimating (too soft) the site periods for the entire range of data, while the EHVSR estimates seem to be more balanced across the period range. This bias is confirmed in Fig. 7a, which displays a box and whisker plot for the percent error values originally computed in Fig. 5. The L&C-1994 contour map tends to overestimate (too soft) the site period for the MHVSR points by 15% on average. However, the L&C-1994 contour map tends to correctly predict the EHVSR points with 0% bias between the estimated and measured site periods (see Fig. 6a and 7b). In contrast, the site period comparison for NTC 2004 in Fig. 6b shows more balanced predictions for the MHVSR data with an underprediction for periods greater than 1.5 sec. This bias is confirmed in Fig. 7a, where a -9% bias is observed in the MHVSR, which is primarily a result of the longer period points in the Xochimilco-Chalco Lake. The EHVSR data, tends to slightly underpredict by -5% as shown in Figure 7b. These estimates for the NTC-2004 match well with results provided by Celebi et al. [26]. For the AEA-2010 comparison in Fig. 6c, the MHVSR points tend to have a bias toward overestimating the site period with an 11% bias observed in Fig. 7a. The EHVSR points in Fig. 6c, tend to be balanced up to a site period of 2.5 sec after which it tends to significantly underpredict the site period. This is likely due to the oversimplification of the deeper part of the basin by AEA-2010, which tended to focus on the eastern edge of the basin. These longer period points also tend to drag the overall EHVSR period estimates toward a -5% bias observed in Fig. 7b. This indicates that the L&C-1994 and AEA-2010 site period maps tend to overpredict the site period for the MHVSR measurements and correctly or slightly overpredict for the EHVSR measurements, while the NTC-2004 site period map tends to underpredict for both MHVSR and EHVSR measurements. In addition, the AEA-2010 map tends to significantly underpredict at longer periods (i.e., the center of the basin). Overall, the NTC-2004 contour map has the best performance at predicting the MHVSR site periods, while the L&C-1994 contour map (followed very closely by the NTC-2004 and AEA-2010 maps) has the best performance at predicting the EHVSR site periods.

Comparing the estimated and measured site periods for the MHVSR and EHVSR in Fig. 7a and b, there is a clear bias of approximately -15% between the site periods estimated using microtremors and earthquake records for the L&C-1994 and AEA-2010, while for the NTC-2004 a bias of +4% is observed. This negative bias (i.e., softening of the site period) when using EHVSR versus MHVSR may be the result of nonlinear site effects (shear modulus reduction) in the earthquake record as opposed to the linear strain range measurements made when using microtremors. While this bias could also be the result of the limited

period range of the MHVSR measurements, the EHVSR data shows a clear negative bias even in the short period range (0.5-2.0 sec) where the MHVSR data is available. Therefore, this is unlikely to be a significant factor. In Fig. 8, the recorded PGA for the 2017 Puebla-Mexico City earthquake from each SMS used for EHVSR is plotted against the percent error for the estimated versus measured site periods using the NTC-2004 site period contour map. From the figure, there is slight downward correlation between larger PGA values and larger bias between the estimated and measured site periods indicating that non-linear site effects may have played a role in the observed bias. However, the trend is very poor with an R squared value of 0.23 indicating a very weak correlation. The lack of nonlinear behavior in the lacustrine clays is supported by resonant column work by Mayoral et al. [4], which showed that due to the high Plasticity Index (PI) of the lacustrine clay deposits in Mexico City, the clays stayed very linear out to high shear strains having very little nonlinear behavior. Other authors have investigated the difference between MHVSR and EHVSR results and suggested a difference in the wavefield (surface wave versus vertically propagating shear waves) contributed to the observed differences between these methods [27]. While the particular cause for this bias cannot be fully explained given the available data, the bias toward longer site periods during strong ground shaking can have a significant influence on the site effects in Mexico City and should be considered in seismic analysis.

3.3 Potential Site Period Changes in Mexico City

As discussed previously, the consolidation of the lacustrine clay deposit in the Mexico City basin is believed to be causing a site period shift across the basin. While the site period change is quite variable across the city, the most significant changes are expected on the western edge of the basin where the majority of the MHVSR measurements were performed in this study [11]. To understand the accuracy of the Arroyo et al. [11] site period change predictions, the site period for each of the MHVSR locations is estimated using the Arroyo et al. [11] contour maps for 1985, 2010, and 2050 along with the L&C-1994 and NTC-2004 maps using the same procedure used to develop Figures 5-7. The average percent error between the estimated and measured MHVSR points are plotted against the year each contour map was developed and is shown in Fig. 9. As expected the percent error estimates from the Arroyo et al. [11] contour maps for 1985, 2010, and 2050 form an excellent linear trend line indicating the accuracy of the site period estimates from each map. Using this trend line, the year where zero bias occurs in the data will be the year (according to the Arroyo et al. [11] estimates) that best represents the measured site periods, which is the year 2043 according to the current dataset. This indicates the site period changes in at least the western portion of the Mexico City basin are progressing faster than estimated by Arroyo et al. [11] as the measurements in this study were taken during 2017. Interestingly, the L&C-1994 percent error is very close to the developed trend line indicating its overall agreement with the site period maps developed by Arroyo

et al. [11]. In contrast, the NTC-2004 contour maps tend to underestimate the site periods resulting in site period estimates which are too stiff compared to the measured site period values. This indicates the NTC-2004 provides the best estimated site periods when using microtremors and likely accounts for future consolidation within the Mexico City basin. However, it also indicates the NTC-2004 map is slightly too stiff in the western region of the basin where testing was conducted.

4.0 Shear Wave Velocity Results

In Fig. 10, the results of the dynamic site characterization measurements are shown for five sites in Mexico City and Puebla where surface wave testing was conducted. The left set of figures contains the experimental dispersion curves and theoretical dispersion curves for the median and 1000 lowest misfit Vs profiles. The middle figures contain the experimental MHVSR curves and theoretical ellipticity curves for the 1000 lowest misfit Vs profiles and median Vs profile. The right figures contain the 1000 lowest misfit Vs profiles along with the median of the 1000 lowest misfit Vs profiles. The Parque España, Escocia, and La Morena sites are all located on the western edge of Mexico City within Lake Texcoco with the Escocia site located in Zone II and the Parque España and La Morena sites located in Zone IIIa (see Fig. 2 and 4). The Gral Tlahuac site is located in the southern portion of Mexico City within the old Lake Xochimilco-Chalco and within Zone IIIb (see Fig. 2 and 4). The final site (Cactopea) is located in Puebla to the Southeast of Mexico City on an area underlined by igneous extrusive rock (see Fig. 2).

Comparing the site periods at each of the sites, the Cactopea site is the only location where an MHVSR peak was not observed. This is likely due to the site being located on igneous extrusive rocks. The Escocia site had the shortest measured site period at 0.93 sec (1.08 Hz), which matches well with its location in Zone II. The Parque España and La Morena sites have similar site periods of 1.35 sec (0.74 Hz) and 1.28 sec (0.78 Hz), respectively, which also agrees with the Zone IIIa designation. The Gral Tlahuac site has the longest period of 2.0 sec (0.5 Hz), which also agrees well with the Zone IIIb designation. During the inversion of each site, the resulting Vs profiles were able to match the experimental MHVSR peak at each site, indicating the robustness of the resulting Vs profiles.

Comparing the dispersion curves and resulting Vs profiles at the sites in Mexico City, each site tended to have a stiff crust overlying a softer presumably clay layer based on the general geology of the area. For the sites in Lake Texcoco, the Vs of the upper clay layer was extremely soft with a Vs of between 50 m/s and 70 m/s. The thickness of this layer varied between 3 and 4 meters at the Escocia site to 10-12 meters at the Parque España and La Morena sites. At each site this very soft clay layer was followed by a stiffer presumably clay layer with a Vs of between 130 m/s and 150 m/s and extending to 37 m, 24 m, and 41 m below the surface at the Parque España, Escocia, and La Morena sites, respectively. At these depths,

the first major impedance contrast is encountered at each site with the depth to this layer matching well with the measured MHVSR site period at each location (i.e., longer site periods equal deeper impedance contrasts). However, the estimated velocity of this stiffer impedance layer is quite variable ranging between 250 m/s and 400 m/s, which is primarily due to the lack of long wavelength data at each site. Therefore, the velocity of the layer is only shown for illustration purposes and should not be relied on for further analysis. Comparing the depth to the major impedance contrast at these sites to the borehole information provided by Arroyo et al. [11], the developed Vs profiles typically have a depth to the first major impedance contrast of 1-4 meters deeper than the depth estimated from the boreholes. This is a reasonable level of accuracy given the boreholes provided in Arroyo et al. [11] were between 0.5 km and 1.5 km from each of the testing locations, which may not be significant in many environments, but given the rapidly changing thickness of the clay layers in Mexico City, we consider the resolved depths to be reasonably accurate. The V_{S30} for each site was between 92 m/s and 136 m/s, which is significantly less than the American Society of Civil Engineering (ASCE) 7 Standard upper limit for site class E of 180 m/s, underscoring the extremely soft soil present in Mexico City. However, all the sites would be site class F given the soft, very high plasticity clays at each location.

For the Gral. Tlahuac site, which is located in Lake Xochimilco-Chalco, a single soft clay layer was resolved below the stiff crustal layer. This indicates the upper layer is stiffer than sites tested in Texcoco Lake (87 m/s versus 50-70 m/s). However, the deeper portion of the clay layer is softer than observed in Texcoco Lake. While the dispersion data at the site shows some signs of a velocity reversal in the subsurface, the simplest solution for the given data is a single 87 m/s layer rather than soft and stiff layer even though a velocity reversal would decrease the misfit between the experimental and theoretical dispersion curves. The single soft clay layer extends to a greater depth than observed at the Lake Texcoco site, which matches well with the longer 2.0 sec site period. The V_{S30} for the site was estimated to be 88 m/s, which is significantly softer than the ASCE 7 site class E boundary similar to the sites in Lake Texcoco.

Compared to the sites in Mexico City, the Cactopea site is significantly stiffer with a V_{S30} of 367 m/s just above the ASCE 7 site class C boundary of 360 m/s. The site consists of a soft to medium stiff surface layer (0-4 meters with Vs of 100-200 m/s) followed by a very stiff soil layer from 4-30.8 meters with a Vs of 425-475 m/s. At 30.8 meters, a potential weathered bedrock layer is encountered at the site. As mentioned above, there was no HVSR peak measured at the site, which could be due to a lack of a strong impedance contrast as indicated by the ellipticity computations based on the developed Vs profiles.

5.0 Conclusions

This study presented dynamic site characterization measurements made in the areas affected by the 2017 Puebla-Mexico City Earthquake. These measurements included Microtremor HVSR (MHVSR) and Earthquake HVSR (EHVSR) measurements made in Mexico City and areas to the south and east of the city and surface wave measurements made in Mexico City and Puebla. The measured site periods from MHVSR were shown to compare well with geologic conditions known to exist in the area. The MHVSR and EHVSR site period measurements were shown to compare well with the NTC [9] geo-seismic map of Mexico City with the zones clearly corresponding well to the general period ranges used to develop the map. The comparison of the site period measurements to previously developed site period contour maps indicated the NTC [9] map provided the best estimate of site periods collected using MHVSR methods (linear strain range) with only a -5% underprediction in the site periods for the measurement locations. However, errors between 30-60% were observed between the estimated and measured sites period for the NTC-2004 map. While the NTC-2004 map provided the best average estimated, the Lermo and Chávez-Garcia [7] site period map provided the most accurate predictions for the EHVSR data. Overall, each contour map was generally within +/- 30% of the measured site period for all the locations, but errors up to 70% were observed at some locations. A comparison of the MHVSR to the Arroyo et al. [11] site period maps from 1985, 2010, and 2050 revealed that the site period in the western portion of the basin maybe changing more rapidly than predicted by Arroyo et al. [11]. However, site period estimates from the NTC [9] map still provides a good estimate of site period across the Mexico City basin with estimates generally within 10% of the measured values.

The Vs profiles collected in the basin agreed well with the depth of clay from borings provided by Arroyo et al. [11] with sites having a stiff crust followed by a very soft clay layer with Vs of approximately 60 m/s in Lake Texcoco and 87 m/s in Lake Xochimilco-Chalco, followed by a slightly stiffer clay layer with Vs of slightly over 140 m/s in Lake Texcoco and 88 m/s in Lake Xochimilco-Chalco until the impedance contrast, which is believed to generate the fundamental site period, is encountered. The Cactopea site located in Puebla was significantly stiffer than any sites in Mexico City with Vs over 400 m/s in most of the layers. Overall, the results of this study reinforce the complex geologic, geotechnical, and hydrogeologic conditions in the Mexico City region emphasizing the need to continue to understand the dynamic site conditions throughout the region due to the continually changing conditions.

6.0 Acknowledgements

This work is based in part on work supported the National Science Foundation through the Geotechnical Engineering Program under Grant Nos. CMMI-1266418 and CMMI-1822482. Any opinion, findings, and conclusions or recommendations expressed in this article are those of the authors and do not

necessarily reflect the view of the NSF. The GEER Association is made possible by the vision and support of the NSF Geotechnical Engineering Program Directors: Dr. Richard Fragaszy and the late Dr. Cliff Astill. GEER members also donate their time, talent, and resources to collect time-sensitive field observations of the effects of extreme events.

We acknowledge and thank the National Autonomous University of Mexico (UNAM) for the resources, space, and personnel provided to the GEER team during this reconnaissance effort. We acknowledge and thank the support given to select UNAM-GEER members by SOCHIGE (Sociedad Chilena de Geotecnia) and their home universities. Strong motion station results presented and discussed in this paper are the products of the instrumentation and processing work of the Seismic Instrumentation Unit at the Institute of Engineering of UNAM. We greatly appreciate UNAM's willingness to release this data early to the UNAM-GEER teams during and immediately following our reconnaissance.

7.0 References

[1] Asimaki, D., Mayoral, J., and Hutchinson, T. (----). Seismology and Strong Ground Motions in the 2017 Puebla-Mexico City Earthquake, *Soil Dynamics and Earthquake Engineering*, (this issue).

[2] Seed H.B., Romo M.P., Sun J., Jaime A., Lysmer J. (1988). The Mexico earthquake of September 19, 1985—Relationships between soil conditions and earthquake ground motions, *Earthquake Spectra* **4** (4), 687–729, doi: 10.1193/1.1585498.

[3] Pestana, J. M., Sancio, R. B., Bray, J. D., Romo, M. P., Mendoza, M. J., Moss, R. E. S., Mayoral, J. M., and Seed, R. B. (2001). "Geotechnical Engineering Aspects of the June 1999 Central Mexico Earthquakes." Earthquake Spectra, 18(3).

[4] Mayoral J.M., Castañon E., Alcántara L., Tepalcapa S. (2016). Seismic response characterization of high plasticity clays, *Soil Dynamics and Earthquake Engineering* **84**: 174–189, doi: 10.1016/j.soildyn.2016.02.012.

[5] Mayoral J.M., Romo M.P., Osorio L. (2008). Seismic parameters characterization at Texcoco lake, Mexico, *Soil Dynamics and Earthquake Engineering* **28** (7): 507–521, doi: 10.1016/j.soildyn.2007.08.004.

[6] Mayoral, J., Asimaki, D., Arduino, P., Franke, K., Hutchinson, T., Ledezma, C., Montalva, G., Wood, C. (----). Site Effects in the Mexico Basin: Past and Present, *Soil Dynamics and Earthquake Engineering*, (this issue).

[7] Lermo, J., Chavez-Garcia, F.J. (1994). Site effect evaluation at Mexico City: Dominant period and relative ampllification from strong motion and microtremor records, Soil Dynamics and Earthquake Engineering 13, 413-423.

[8] Gurler, E.D., Nakamura, Y., Saita, J.,Sato, T. (2000). Local site effect of Mexico City based on microtremor measurement. 6th International Conference on Seismic Zonation. Palm Spring Riviera Resort, California, USA, pp. 65.

[9] Gobierno del Distrito Federal México (2004). Normas Técnicas Complementarias sobre Criterios y Acciones para el Diseño Estructural de las Edificaciones (NTC-2004).

[10] Hayashi, K., Nozu, A., Tanaka, M., Suzuki, H., and Ovando Shelley, E. (2011) Joint inversion of three-component microtremor measurements and microtremor array measurements at Mexico City. SEG Technical Program Expanded Abstracts 2011: pp. 917-921. https://doi.org/10.1190/1.3628222

[11] Arroyo, D., Ordaz, M., Ovando-Shelley, E., Guasch, J. , Lermo, J., Perez, C., Alcantara, L., Ramı´rez-Centeno, M. (2013), "Evaluation of the change in dominant periods in the lake-bed zone of Mexico City produced by ground subsidence through the use of site amplification factors." Soil Dynamics and Earthquake Engineering 44 (2013), pp. 54-66.

[12] Ovando, E. and Romo, M. P. (1991), "Estimaci6n de Ia velocidad deondas S en Ia arcilla de Ia ciudad de Mexico con ensayos de co no" ,Sismodiruimica, 2, 107-123

[13] Nakamura, Y., (1989). A method for dynamic characteristics estimation of subsurface using microtremor on the ground surface, Rep. Railway Tech. Res. Inst., Jpn 30, 1, 2533.

[14] SESAME, (2004). Guidelines for the implementation of the H/V spectral ratio technique on ambient vibrations: measurements, processing and interpretation, 62 pp.,http://sesamefp5.obs.ujfgrenoble.fr/Delivrables/Del-D23

[15] Molnar, S., Cassidy, J., Castellaro, S., Cornou, C., Crow, H., Hunter, J., Matsushima, S., Sánchez‐Sesma, F., Yong, A. (2018). Application of Microtremor Horizontal‐to‐Vertical Spectral Ratio (MHVSR) Analysis for Site Characterization: State of the Art, Surv Geophys https://doi.org/10.1007/s10712-018-9464-4

[16] Chatelain JL, Guillier B. (2013) Reliable Fundamental Frequencies of Soils and Buildings Down to 0.1 Hz Obtained from Ambient Vibration Recordings with a 4.5-Hz Sensor. Seismological Research

Letters 2013; 84(2): 199-209.

[17] Wathelet, M. (2008). An improved neighborhood algorithm: parameter conditions and dynamic scaling. Geophysical Research Letters, 35, L09301, doi:10.1029/2008GL033256.

[18] Park, C. B., Miller, R. D. & Xia, J. (1999) Multichannel analysis of surface waves, Geophysics, 64: 800-880.

[19] Tokimatsu, K., K. Shinzawa, and S. Kuwayama (1992). "Use of shortperiod microtremors for VS profiling". J. Geotech. Eng. 1992: 118(10), 1544–1588.

[20] Zywicki, D. J., 1999. Advanced Signal Processing Methods Applied to Engineering Analysis of Seismic Surface Waves, Ph.D. Dissertation, School of Civil and Environmental Engineering, Georgia Institute of Technology, Atlanta, GA.

[21] Cox, B. and Wood, C., (2011). Surface Wave Benchmarking Exercise: Methodologies, Results and Uncertainties, GeoRisk 2011: Geotechnical Risk Assessment and Management (C.H. Juang et al., eds.), ASCE GSP 224, 845-852.

[22] Wood, C. and Baker, E. (2018). Potential Cost-Savings of Implementing Site-Specific Ground Motion Response Analysis Results in Design of Mississippi Embayment Bridges, Earthquake Spectra (https://doi.org/10.1193/120517EQS247M).

[23] Deschenes, M., Wood, C., Wotherspoon, L., Bradley, B., Thomson, E. (2018), Development of Deep Site Specific Shear Wave Velocity Profiles in the Canterbury Plains, New Zealand, Earthquake Spectra (https://doi.org/10.1193/122717EQS267M).

[24] Hutchinson, T., Arduino, P., Dafni, J., Martinez-Vela, A., Meneses, J., Mohtar, C., Montgomery, J. (----). Transitioning towards the Epicenter: Damage Mapping in Morelos and Puebla, Soil Dynamics and Earthquake Engineering, (this issue).

[25] Chavez-Garcia, F., Cuenca, J., Lermo, J., Mijares, H. (1995). Seismic Microzonation of the City of Puebla, Mexico. 1995 International Conferences on Recent Advances in Geotechnical Earthquake Engineering and Soil Dynamics. 1. http://scholarsmine.mst.edu/icrageesd/03icrageesd/session07/1

[26] Celebi, M., Sahakian, V., Melgar, D., Quintanar, L. (2018). The 19 September 2017 M 7.1 Puebla-Morelos Earthquake: Spectral Ratios Confirm Mexico City Zoning, BSSA, doi: 10.1785/0120180100

[27] Kawasw, H., Mori, Y., Nagashima, F. (2017). Difference of horizontal-to-vertical spectral ratios of observed earthquakes and microtremors and its application to S-wave velocity inversion based on the diffuse field concept, Earth, Planets and Space 70 (1), https://doi.org/10.1186/s40623-017-0766-4

Table 1. Sites in Mexico where HVSR and surface wave measurements were made along with measured site period and Vs30 results.

Site Name	Latitude	Longitude	Site Period (sec)	V_{S30} (m/s)	Collector
Parque España	19.41546	-99.17138	1.35	92	Uark
H/V 1	19.41456	-99.17408	1.09	-	Uark
H/V 2	19.41294	-99.17477	1.04	-	Uark
H/V 3	19.41148	-99.17576	0.94	-	Uark
H/V 4	19.40897	-99.17729	0.91	-	Uark
Escocia	19.38744	-99.16342	0.93	136	Uark
La Morena	19.39861	-99.15873	1.28	93	Uark
Paseo las Galias	19.32139	-99.09711	1.09	-	Uark
Siracusa	19.31488	-99.09401	-	-	Uark
Del Mar	19.28838	-99.06356	2.00	-	Uark
Av Siren	19.28510	-99.05783	1.67	-	Uark
Hospital Gral Tlahuac	19.28735	-99.05354	2.00	88	Uark
Rancho	19.30449	-99.12294	1.00	-	Uark
Ruta 1	19.31511	-99.09303	1.63	-	Uark
Cuernavaca	18.92623	-99.23206	1.14	-	Uark
Emilino Zapata	18.84108	-99.18321	0.09	-	Uark
Jojutla	18.61443	-99.17948	0.27	-	Uark
Treinta	18.69678	-99.17749	-	-	Uark
Yautepec Bridge	18.73045	-99.11992	0.83	-	Uark
Tlatizapan	18.68380	-99.11741	-	-	Uark
Tlaquiltenango	18.62925	-99.16080	-	-	Uark
City Plaza	19.04354	-98.19788	0.78	-	Uark
Calle 6	19.04371	-98.19273	0.89	-	Uark
Cactopea	19.01498	-98.25871	-	367	Uark
F01	19.41258	-99.18377	0.73	-	UdeC-PUC
F02	19.41132	-99.17998	0.87	-	UdeC-PUC
F03	19.41136	-99.17856	0.88	-	UdeC-PUC
F04	19.41139	-99.17790	0.88	-	UdeC-PUC
F05	19.41139	-99.17751	0.93	-	UdeC-PUC
F06	19.41139	-99.17688	0.95	-	UdeC-PUC
F07	19.41141	-99.17582	0.91	-	UdeC-PUC
F08	19.41143	-99.17525	1.00	-	UdeC-PUC
F09	19.41145	-99.17482	1.01	-	UdeC-PUC
F10	19.41145	-99.17441	0.90	-	UdeC-PUC
F11	19.41146	-99.17232	1.19	-	UdeC-PUC
F12	19.41147	-99.17164	1.16	-	UdeC-PUC
F13	19.41267	-99.17084	1.16	-	UdeC-PUC
F14	19.41149	-99.17051	1.16	-	UdeC-PUC
F15	19.41131	-99.16984	1.11	-	UdeC-PUC
F16	19.41017	-99.16619	1.25	-	UdeC-PUC
F17	19.41090	-99.16446	1.22	-	UdeC-PUC
F18	19.41112	-99.16336	1.21	-	UdeC-PUC

Notes: - indicates no site period was resolved at the site or that Vs measurements were not taken at the site. Uark is University of Arkansas and UdeC-PUC is Universidad de Concepción and Pontificia Universidad Católica de Chile.

Table 2. Site period estimates using EHVSR for station motion station records from the 2017 Puebla-Mexico City EQ. PGA and estimated HVSR site period of each record is provided along with station location and station code.

Station Code	Latitude	Longitude	Site Period (sec)	PGA (g)
AE02	19.4313	-99.0589	NA	0.117
AL01	19.4356	-99.1453	1.92	0.119
AO24	19.3580	-99.1539	1.20	0.122
AP68	19.3817	-99.1076	NA	0.137
AU11	19.3963	-99.0866	4.17	0.092
AU46	19.3832	-99.1681	1.05	0.097
BA49	19.4097	-99.1450	2.33	0.115
BL45	19.4253	-99.1481	1.72	0.116
BO93	19.4662	-99.1051	2.93	0.097
CA59	19.4268	-99.1188	2.56	0.092
CCCL	19.4498	-99.1370	1.85	0.087
CE18	19.3385	-99.0852	NA	0.074
CE23	19.4630	-99.0610	4.34	0.061
CE32	19.3847	-99.0540	NA	0.082
CH84	19.3300	-99.1254	1.39	0.230
CI05	19.4186	-99.1653	1.39	0.116
CJ04	19.4097	-99.1567	1.79	0.114
CO47	19.3714	-99.1703	1.00	0.096
CO56	19.4215	-99.1590	2.27	0.116
CS78	19.3662	-99.2264	2.40	0.089
CU80	19.2945	-99.1039	NA	0.171
CUP5	19.3302	-99.1811	1.30	0.060
DM12	19.4333	-99.0972	3.00	0.093
DX37	19.3322	-99.1439	1.15	0.192
EO30	19.3885	-99.1772	0.61	0.084
ES57	19.4025	-99.1779	1.00	0.086
FJ74	19.2990	-99.2100	1.30	0.094
GA62	19.4385	-99.1401	2.04	0.099
GC38	19.3161	-99.1059	1.72	0.128
GR27	19.4756	-99.1802	1.00	0.122
HJ72	19.4251	-99.1301	2.22	0.098
IB22	19.3459	-99.1301	NA	0.164
JA43	19.4064	-99.1257	2.38	0.108
JC54	19.3130	-99.1272	1.20	0.224
LEAC	19.3227	-99.0976	1.70	0.199
LI33	19.3064	-98.9631	2.09	0.141
LI58	19.4263	-99.1569	2.00	0.098

LV17	19.4937	-99.1278	2.08	0.125
ME52	19.4392	-99.1821	NA	0.073
MI15	19.2834	-99.1253	1.50	0.211
MT50	19.4262	-99.1904	1.00	0.059
MY19	19.3461	-99.0433	2.78	0.122
NZ20	19.3934	-99.0016	4.00	0.149
NZ31	19.4178	-99.0253	5.10	0.112
PCJR	19.4228	-99.1591	2.17	0.101
PD42	19.4064	-99.1000	4.00	0.098
PE10	19.3903	-99.1324	2.00	0.127
PISU	19.4857	-99.0490	4.50	0.099
RM48	19.4359	-99.1280	2.13	0.080
SCT	19.3947	-99.1487	1.69	0.093
SI53	19.3753	-99.1483	1.43	0.181
TACY	19.4045	-99.1952	NA	0.064
TH35	19.2786	-99.0000	3.80	0.194
TL08	19.4500	-99.1336	1.72	0.085
TL55	19.4536	-99.1425	1.75	0.084
TP13	19.2922	-99.1708	4.00	0.068
UC44	19.4337	-99.1654	1.45	0.127
UI21	19.3700	-99.2642	NA	0.081
VC09	19.4548	-99.1228	2.10	0.122
VM25	19.3815	-99.1253	2.27	0.097
X036	19.2716	-99.1027	NA	0.177
XP04	19.4198	-99.1353	2.33	0.110

Table 3. Median shear wave velocity profiles from inversion for each site in this study.

Parque Espana		**Escocia**		**La Morena**		**Hospital Gral Tlahuac**		**Cactopea**	
Vs (m/s)	Depth (m)	Vs (m/s)	Depth (m)	Vs (m/s)	Depth (m)	Vs (m/s)	Depth (m)	Vs (m/s)	Depth (m)
115	2	700	0.13	220	1	600	0.3	121	1.6
70	4	112	2	50.5	5.7	300	0.4	203	4
60.5	14.4	67	5.3	69	12.3	87	49.8	436	10.3
146.4	37.2	146	24	136	40.8	250	>50	457	16.7
388	>60	231	>30	396	>50			471	30.8
								757	35.1
								795	>60

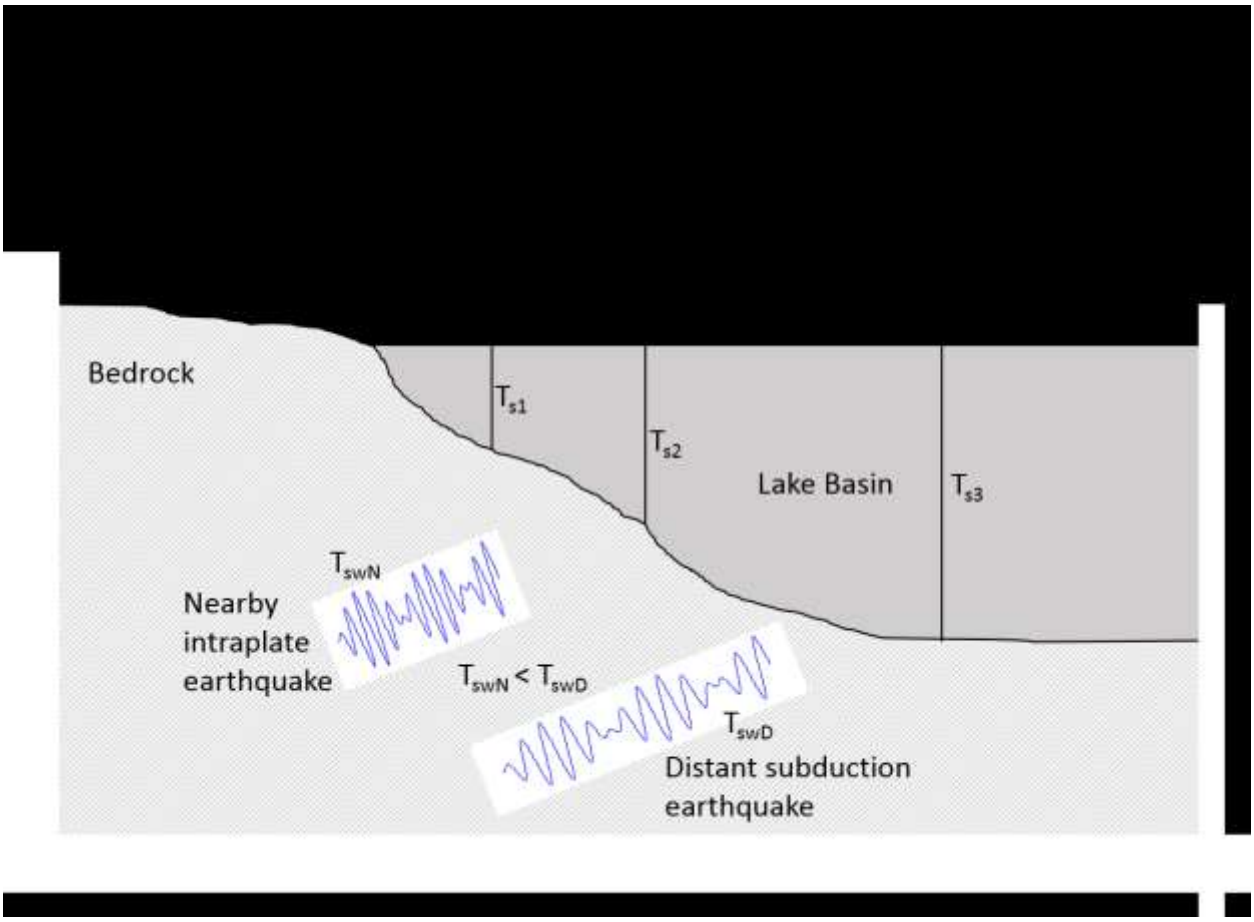

Fig. 1. Illustration of the Mexico City basin comparing the predominant period of distant subduction (TswD) and near intraplate (TswN) seismic sources, natural period of the soil column (Ts) in various areas of the basin, and natural period of buildings (Tb) most likely to be affected in different part of the basin.

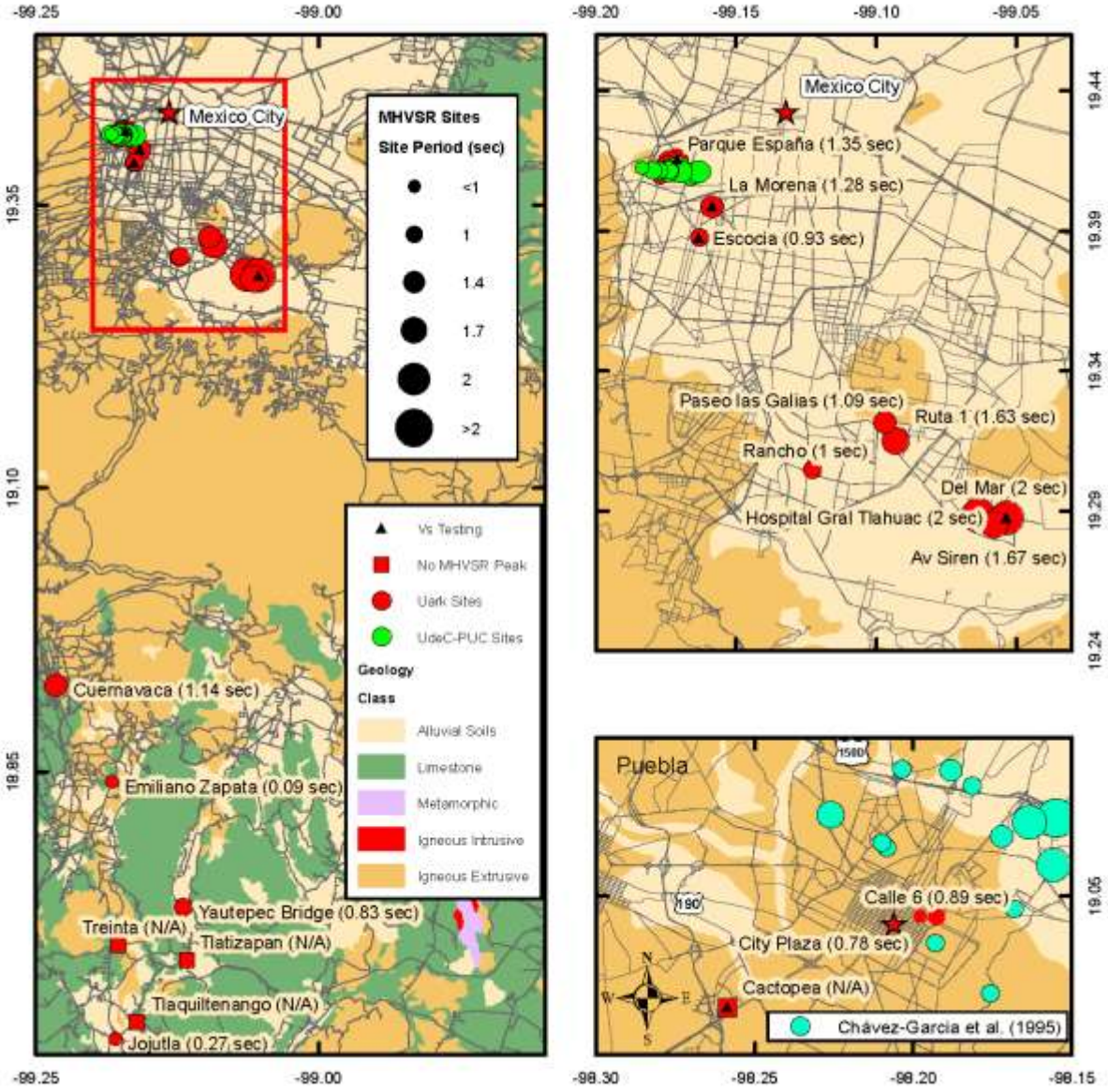

Fig. 2. Location map for site period and surface wave measurements made in Mexico City, the state of Morelos, and Puebla overlain on geologic map of the area from INEGI. For the subarea of Puebla, site periods from [23] are shown for comparison.

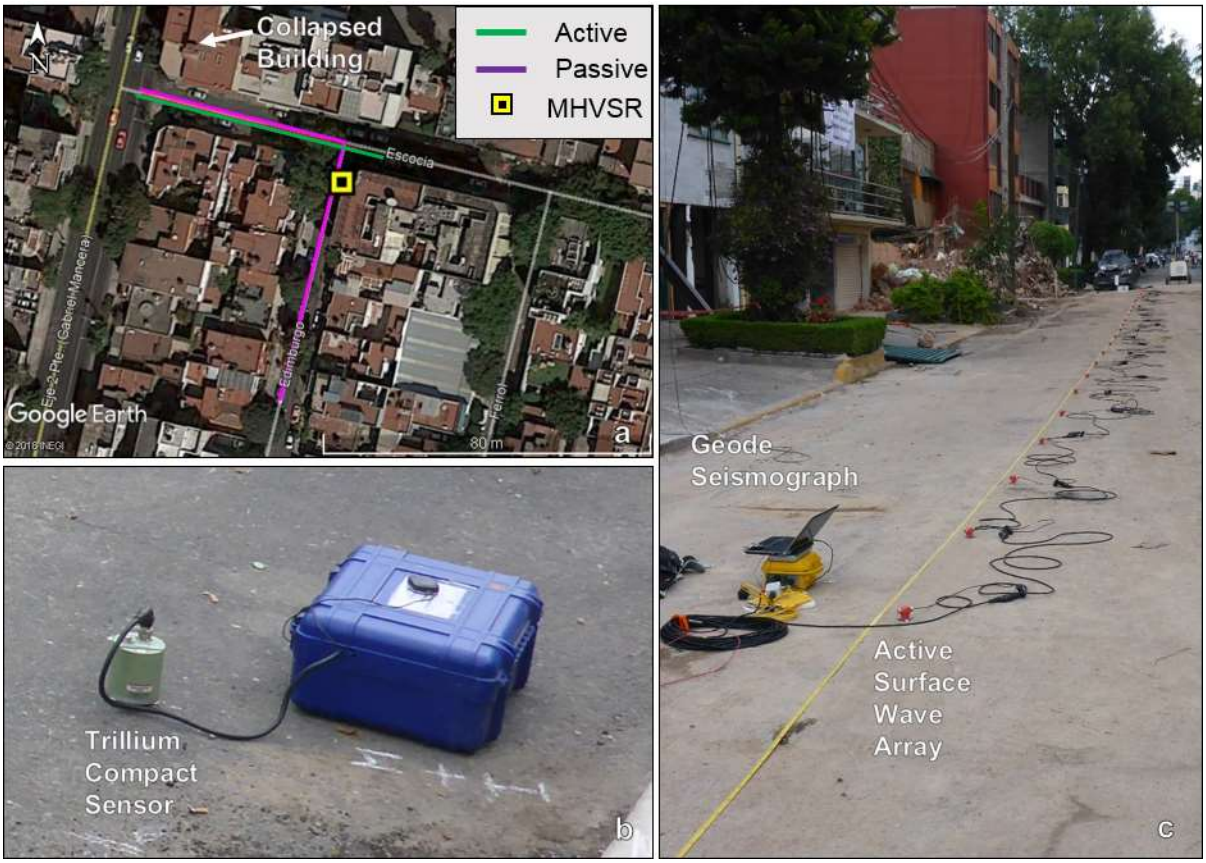

Fig. 3. Example dynamic site characterization setup at Escocia. a) Plan view of active and passive array used for testing along with HVSR location, b) HVSR sensor used for testing, c) active surface wave array used during testing.

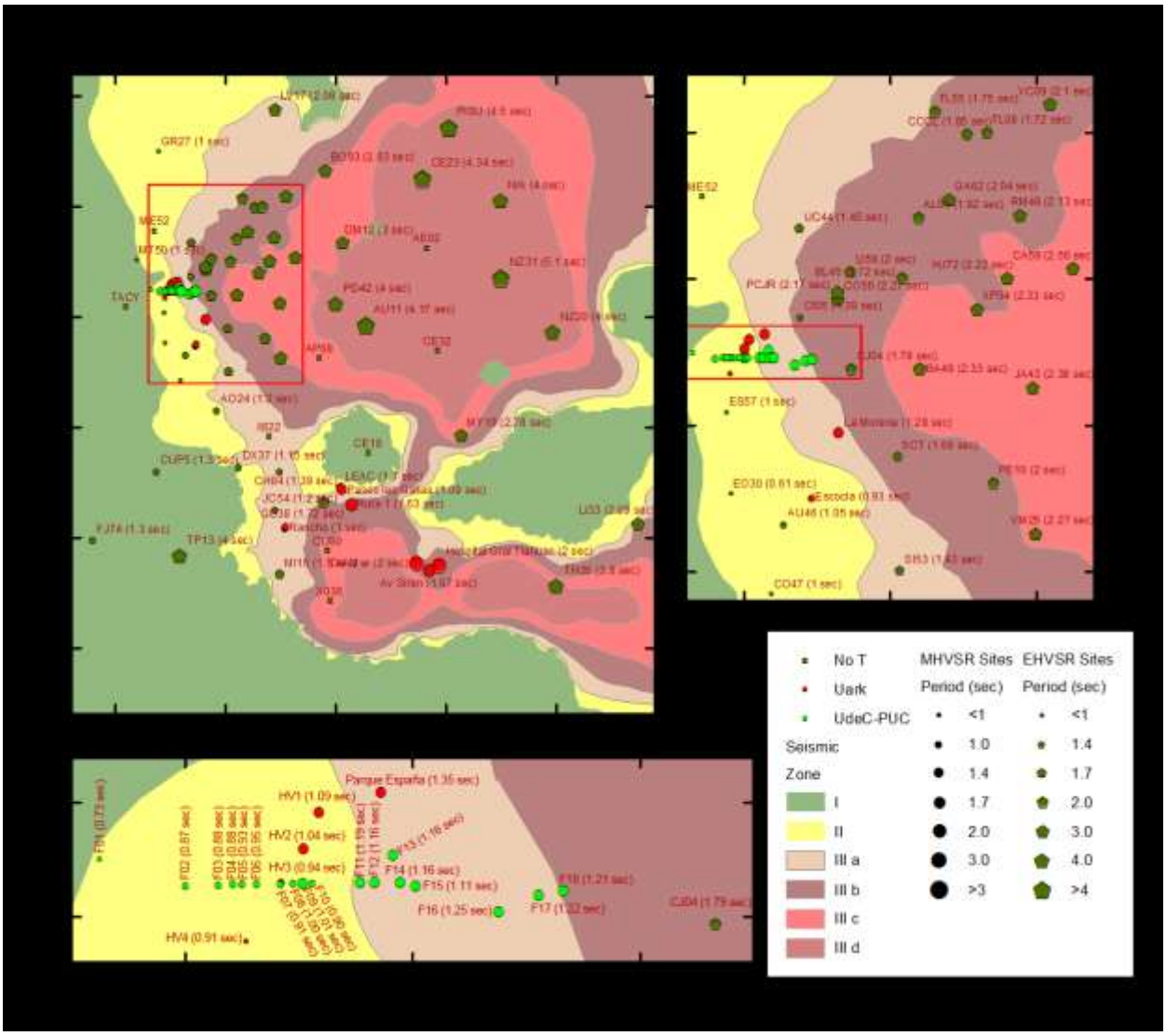

Fig. 4. Comparison map of geo-seismic zonation map of Mexico City from NTC [9] and fundamental site periods calculated using MHVSR and EHVSR methods in Mexico City.

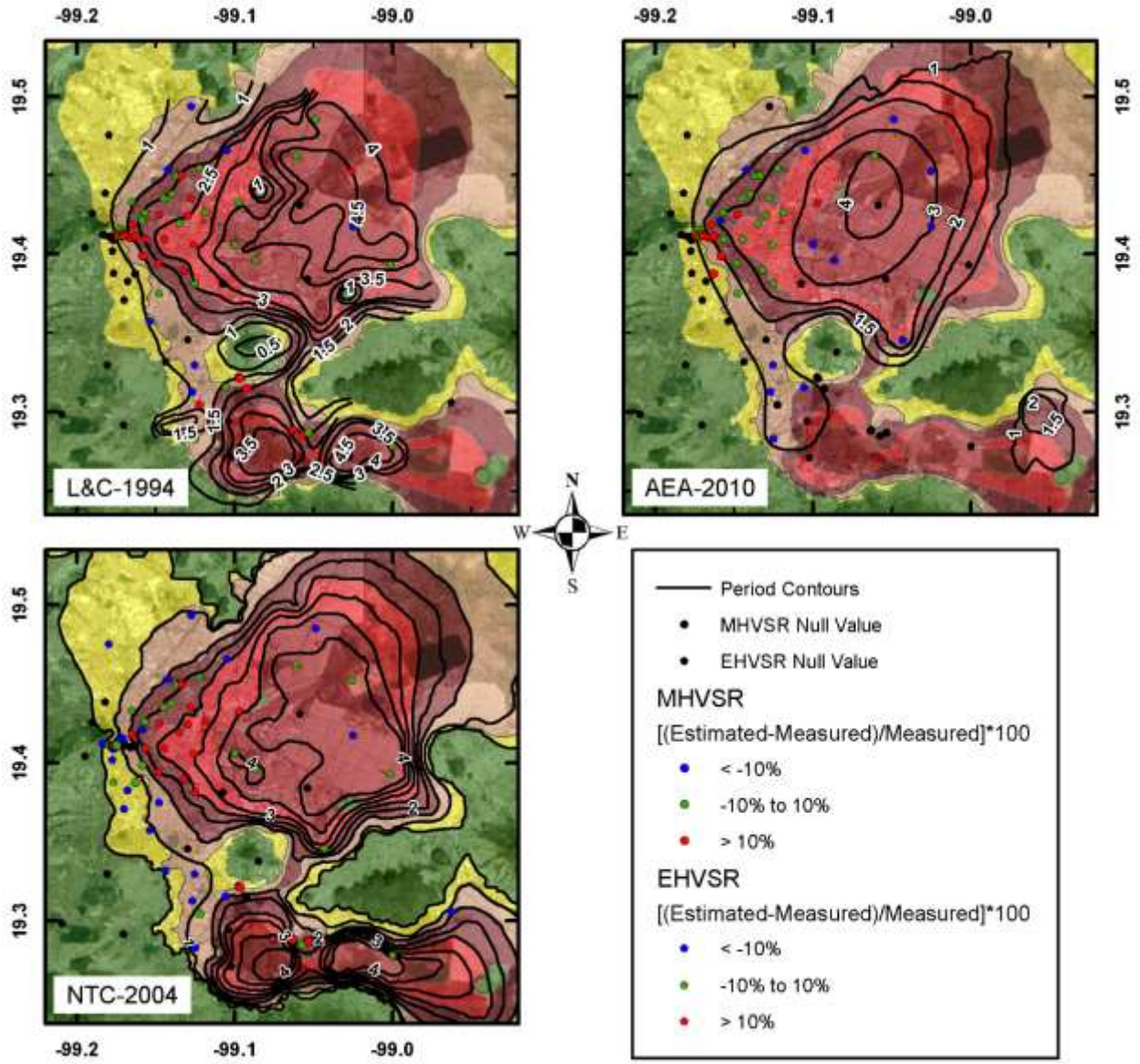

Fig. 5. Comparison of site periods from MHVSR and EHVSR to site period contour maps published by Lermo and Chávez-Garcia [7], NTC [9], and Arroyo et al. [11] (2010 estimate).

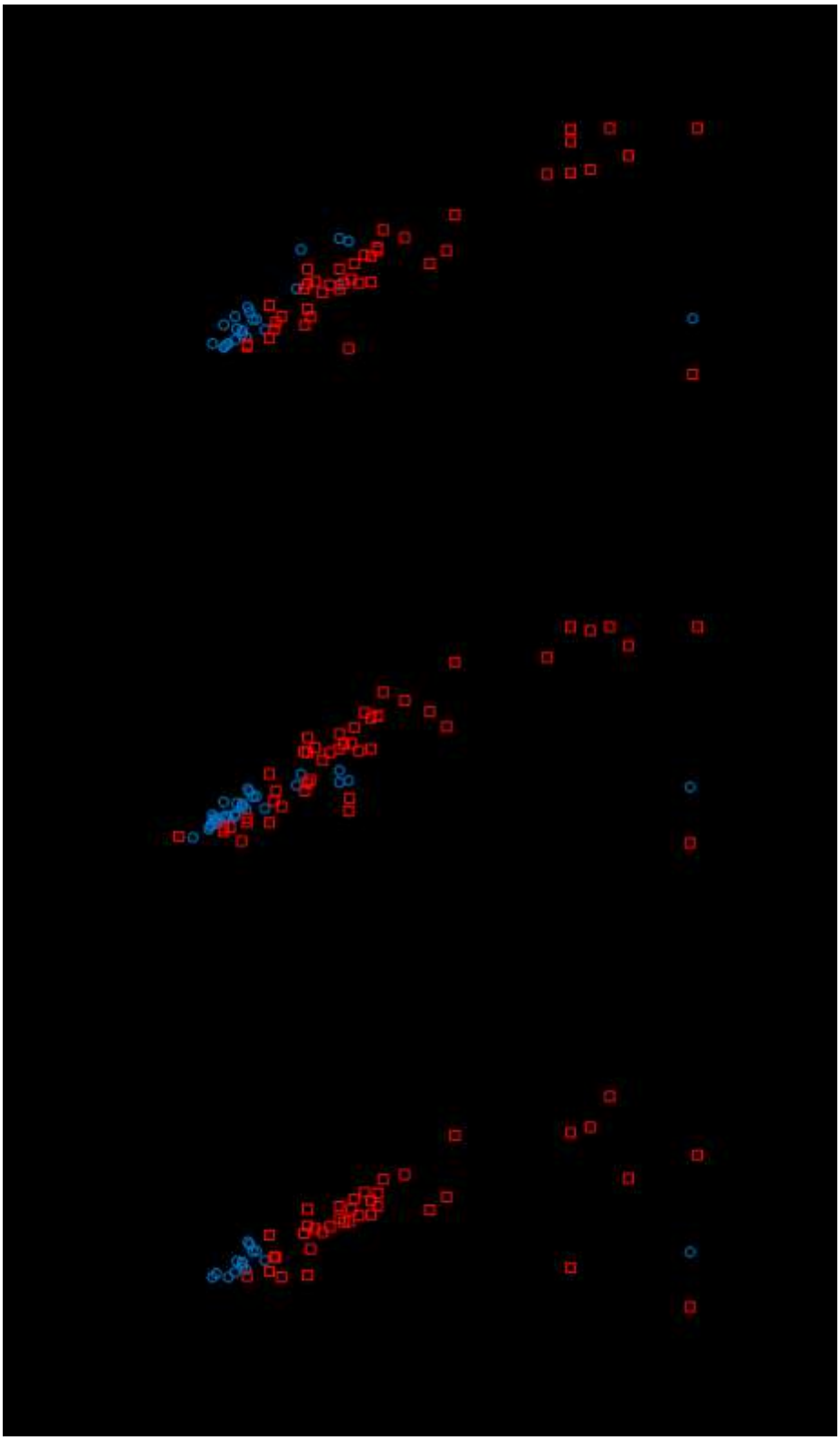

Fig. 6. Estimated bias error between site periods measured using MHVSR and EHVSR and those estimated based on the contour maps by a) Lermo and Chávez-Garcia [7], b) NTC [9], and c) Arroyo et al. [11] (2010 estimate) for the same measurement locations.

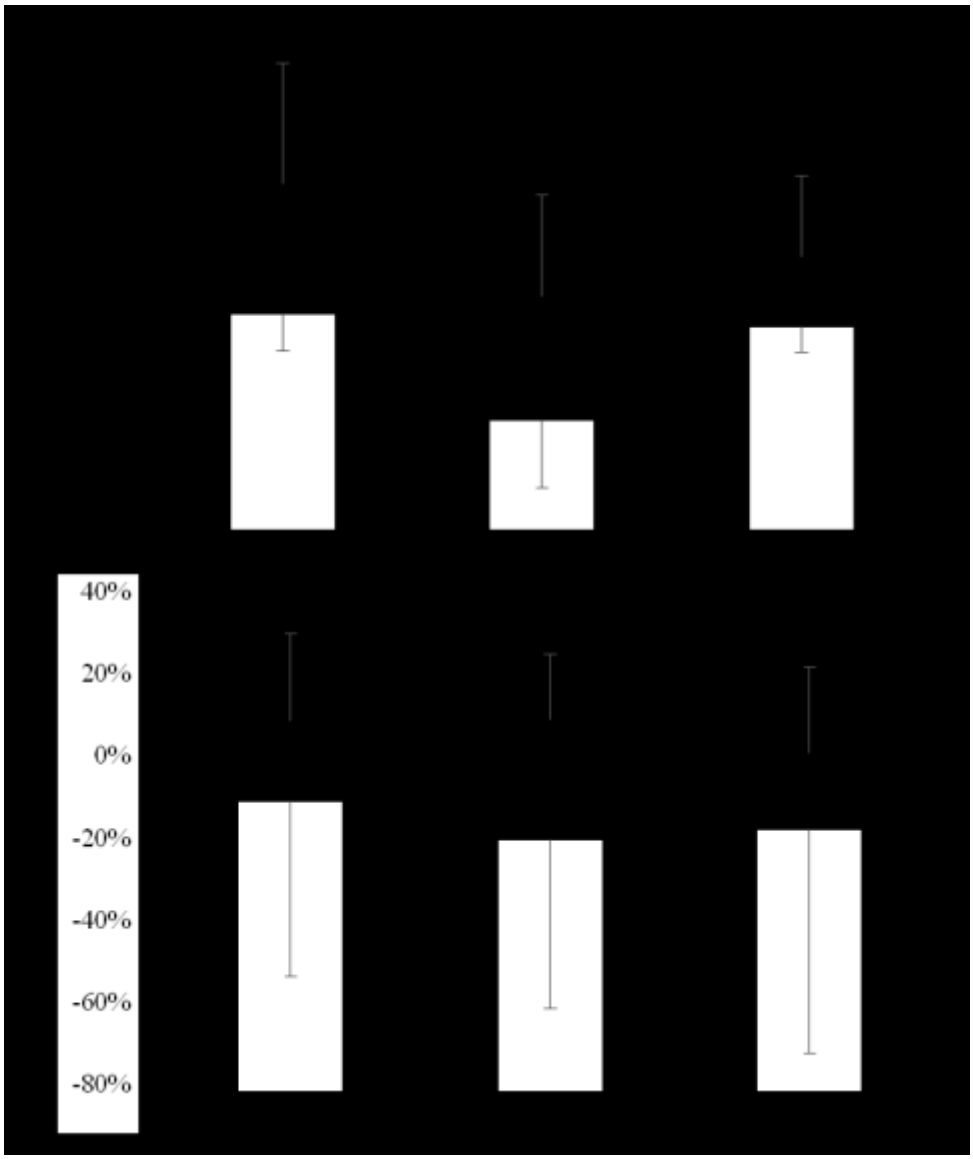

Fig. 7. Box and whisker plot of the percent error between the a) MHVSR and b) EHVSR site period measurements and estimated site periods from the Lermo and Chávez-Garcia [7], NTC [9], and Arroyo et al. [11] (2010 estimate) contour maps.

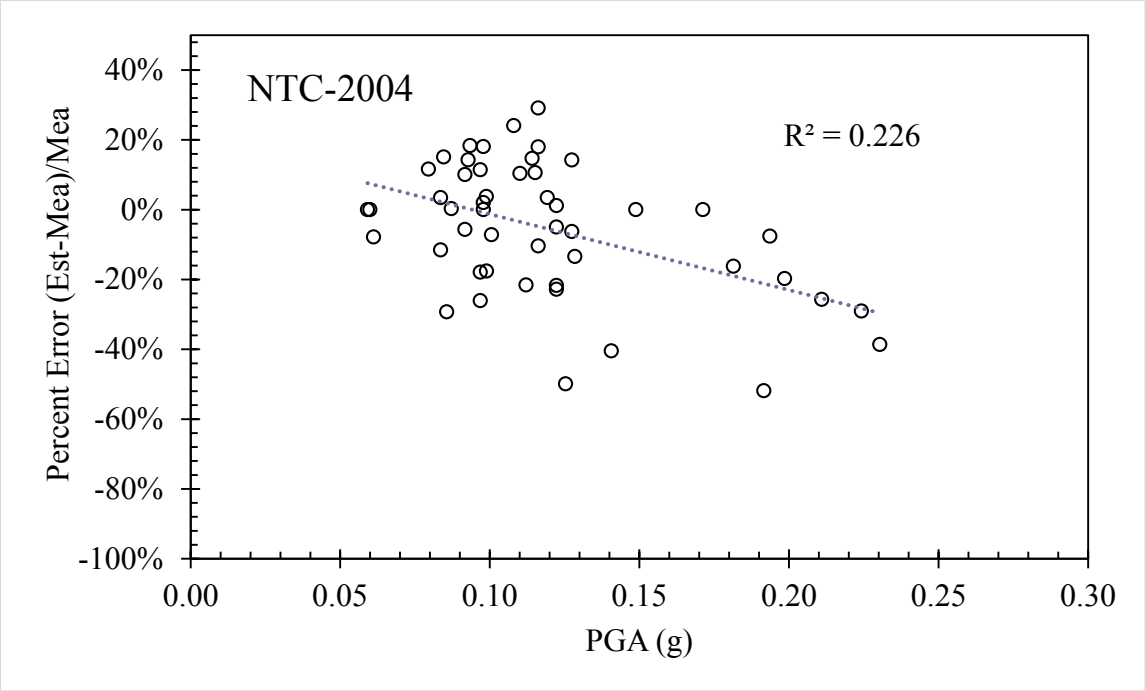

Fig. 8. Comparison of percent error between the EHVSR measured site periods and estimated site periods for the NTC [9] and the recorded PGA at each SMS location.

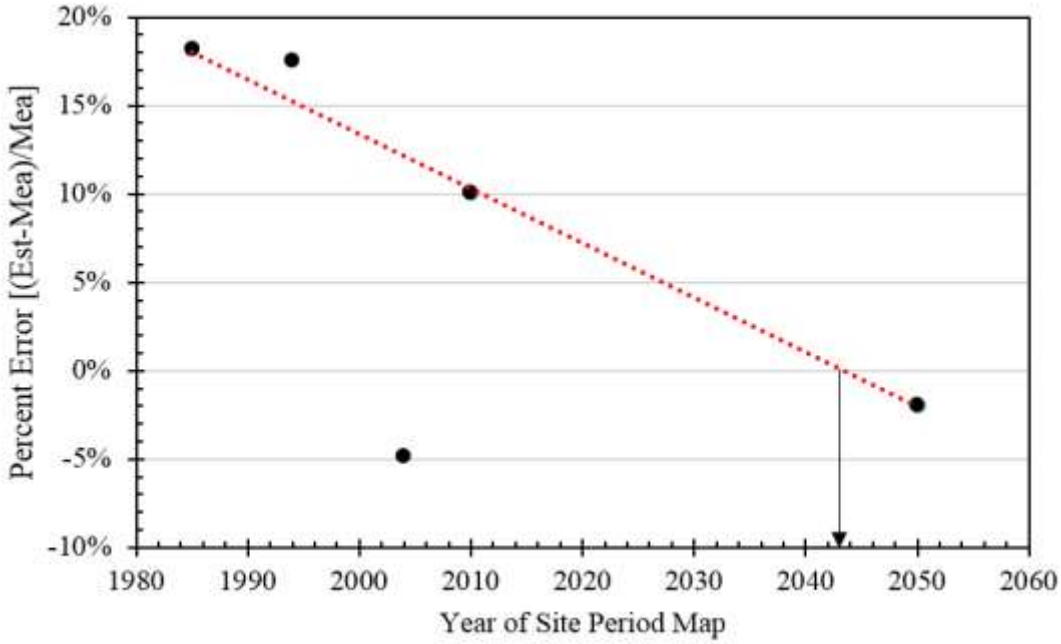

Fig. 9. Comparison of percent error between the MHVSR measured and estimated site periods for the Arroyo et al. [11] estimates for 1985, 2010, and 2050 along with the Lermo and Chávez-Garcia [7], and NTC [9] percent errors. The vertical arrow indicates in which year zero bias is reached.

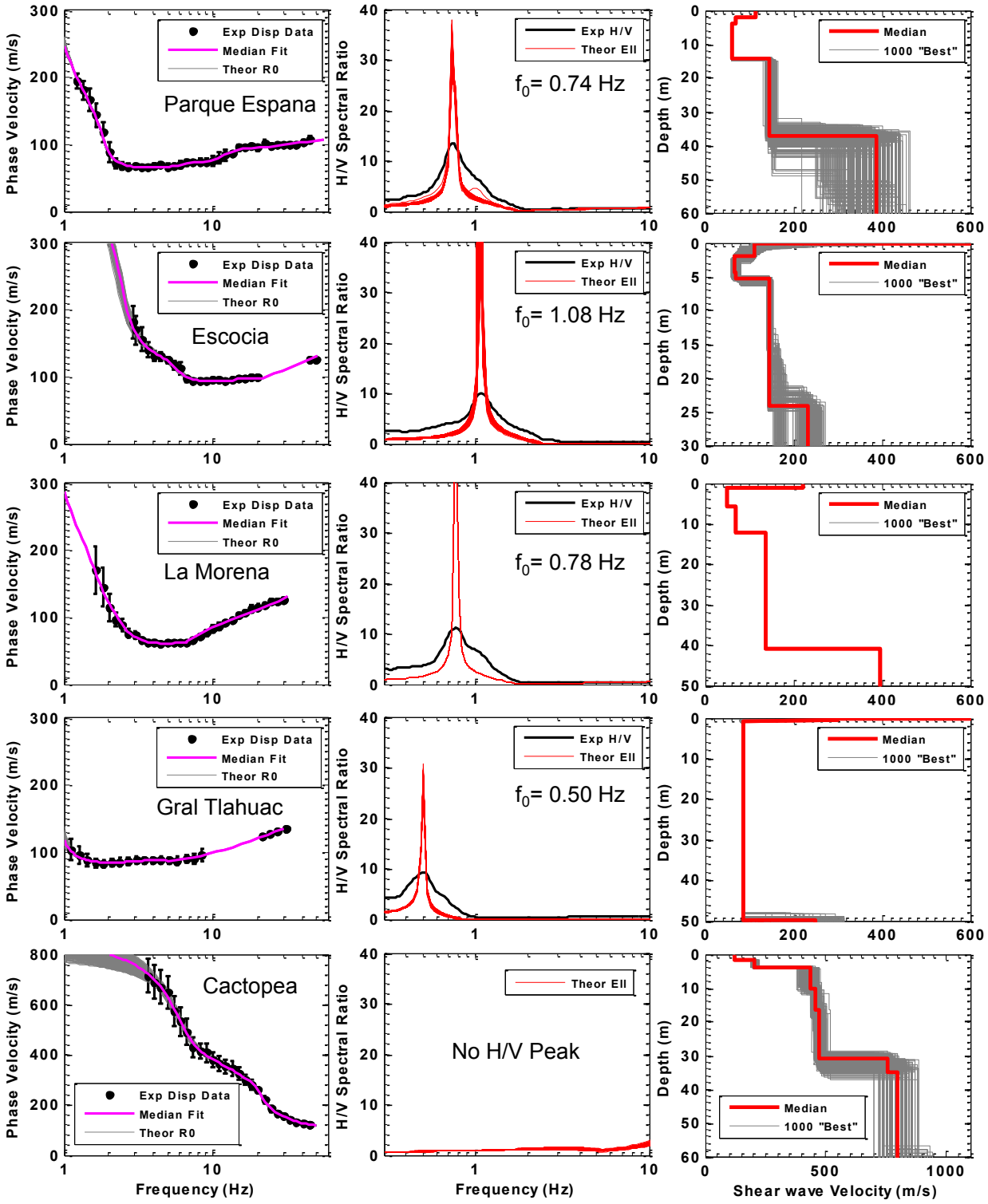

Fig. 10. Dynamic site characterization results: Left) experimental dispersion curves and theoretical dispersion curves for the median and 1000 lowest misfit Vs profiles. Middle) experimental HVSR curve and theoretical ellipticity curves for 1000 lowest misfit Vs profiles and median Vs profile. Right) 1000 lowest misfit Vs profiles along with the median of the 1000 lowest misfit Vs profiles. Note: the scales may change for each site as some sites are vastly stiffer than others.